RESEARCH ARTICLE

**ADVANCED
ENERGY & SUSTAINABILITY
RESEARCH**
Open Access
www.advenergysustres.com

Extensive Screening of Solvent-Linked Porous Polymers through Friedel–Crafts Reaction for Gas Adsorption

Vepa Rozyyev, Yeongran Hong, Mustafa S. Yavuz, Damien Thirion, and Cafer T. Yavuz*

Scalability, cost, and feasibility of porous structures in gas capture are prerequisites for emerging materials to be promising in the industry. Herein, a simpler variant of Friedel–Crafts' synthesis of highly porous covalent organic polymers (COPs) based on an unprecedented solvent-mediated crosslinking is presented. Alkyl chlorides behave as both solvents and linkers in the presence of AlCl$_3$. Studies on three classes of 18 different monomers using dichloromethane, chloroform, and 1,2-dichloroethane lead to producing 29 new COPs (124−152). Polymers are characterized by Fourier-transform infrared spectroscopy (FTIR), nuclear magnetic resonance (NMR) spectroscopy, elemental composition analysis, scanning electron microscope (SEM), thermogravimetric analysis (TGA), and porosity analyzer. The synthesized COPs exhibit structures from nonporous to highly porous morphologies with Brunauer–Emmett–Teller (BET) surface areas as high as 1685 m^2 g^{-1}. These COPs show high gas uptake toward CO$_2$ (up to 4.71 mmol g^{-1} at 273 K, 1.1 bar), CH$_4$ (up to 1.31 mmol g^{-1} at 273 K, 1.1 bar), and H$_2$ (up to 2.02 wt% at 77 K, 1.1 bar). The findings point to significant potential in producing sustainable porous materials through simple and scalable methodology developed here.

1. Introduction

Porous solids with high surface areas, thermal stability, and chemically robust nature have attracted great attention because of their applications in gas capture and storage,[1] water treatment,[2] and catalysis.[3] In addition to the commonly used porous materials in the industry such as zeolites, activated carbons, and molecular sieves, recent developments show that various classes of new porous solids have emerged, such as metal organic frameworks (MOFs),[4] covalent organic frameworks (COFs),[5] covalent organic polymers (COPs),[6] hypercross-linked polymers (HCPs),[3e,7] microporous organic polymers (MOPs),[8] porous aromatic frameworks (PAFs),[9] porous polymer networks (PPNs),[10] and benzimidazole-linked polymers (BILPs).[11] To be used in industrial scale, these materials are expected to be highly porous, thermally and chemically robust, and easily synthesized from inexpensive precursors. Although numerous materials have been reported so far, most have drawbacks such as difficult synthetic procedures, expensive and complex starting monomers, or require rare earth metals. So far, only a handful of these porous materials have proven relatively scalable with affordable synthesis.[12]

Considering the availability of the precursors and reagents, Friedel–Crafts (FC) alkylation[13] is one of the most promising

V. Rozyyev
Pritzker School of Molecular Engineering
University of Chicago
5640 South Ellis Avenue, Chicago, Illinois 60637, USA

V. Rozyyev, Dr. M. S. Yavuz, Dr. D. Thirion, Prof. C. T. Yavuz
Graduate School of EEWS
Korea Advanced Institute of Science and Technology (KAIST)
291 Daehak-ro, Yuseong-gu, Daejeon 34141, Republic of Korea

Dr. Y. Hong, Prof. C. T. Yavuz
Department of Chemical and Biomolecular Engineering
KAIST
291 Daehak-ro, Yuseong-gu, Daejeon 34141, Republic of Korea

Dr. M. S. Yavuz
Innvotek Limited
43 Berkeley Square, Mayfair, London W1J 5FJ, UK

Prof. C. T. Yavuz
Advanced Membranes and Porous Materials Center (AMPM)
Physical Sciences and Engineering (PSE)
King Abdullah University of Science and Technology (KAUST)
Thuwal 23955-6900, Saudi Arabia
E-mail: cafer.yavuz@kaust.edu.sa

Prof. C. T. Yavuz
KAUST Catalysis Center (KCC)
Physical Science & Engineering (PSE)
King Abdullah University of Science and Technology (KAUST)
Thuwal 23955, Saudi Arabia

ADVANCED
SCIENCE NEWS
www.advancedsciencenews.com

ADVANCED
ENERGY & SUSTAINABILITY
RESEARCH
Open Access
www.advenergysustres.com

synthetic methodologies for making highly porous networks with stable C—C-bonded frameworks. Since the early works by Davankov et al.[14] to make porous resins, the method was widely adapted to offer HCPs and MOPs. The applications vary from simple gas capture and storage[12d] to catalysis.[15]

In FC alkylation reactions, inexpensive Lewis acids such as aluminum chloride (AlCl₃) and iron chloride (FeCl₃) and chlorinated solvents such as 1,2-dichloroethane (DCE), dichloromethane (DCM), and chloroform (CHCl₃) are commonly used. Although FeCl₃ works fine, using highly reactive AlCl₃ with chlorinated solvents must be controversial as there is a great chance of participation in the FC reaction.[16] Despite these reactivity concerns, several reports used AlCl₃ as a Lewis acid and chlorinated solvents as a solvent.[17] Previously, we showed that chlorinated solvents not only readily participate in FC reactions, but they can produce highly porous network polymers with aromatic monomers in the presence of AlCl₃.[18] In principle, common chlorinated solvents serve as both linkers and solvent. Surprisingly, excess linkers produced network structures, an observation that can only be explained by the formation of highly reactive intermediates. Here, we extend the scope of this chemistry and studied three classes of 18 monomers under the solvent-mediated FC conditions. We then analyzed their gas adsorption properties in great detail. The porous networks show high uptake for carbon dioxide (CO_2), hydrogen (H_2), and methane (CH_4) gases. The method developed here is one of the most affordable FC reactions so far and one of the simplest for the formation of highly porous polymers. Because the reaction takes place rapidly at ambient conditions and uses inexpensive precursors, they will ultimately become the most promising candidates for the gas capture and separation at industrial scales.

2. Results and Discussion

2.1. Synthesis

The alkyl-chlorinated solvents and highly reactive AlCl₃ have readily been used in a number of reports that feature FC reactions or Scholl-type aromatic couplings.[17] We suspected that the solvent may not stay inert and will react with aromatics. Hence, benzene and anhydrous AlCl₃ were reacted at room temperature in 1,2-dichloroethane (DCE), dichloromethane (DCM), and chloroform (CHCl₃) solvents. The precipitates formed in all three solvents and they were insoluble in both water and organic solvents. Getting insoluble products was surprising, as chlorinated solvents were used in excess and the products were expected to be multisubstituted benzenes that are readily soluble in organic solvents. However, the reactions yielded high-molecular-weight network polymers rather than soluble molecules, an observation that can only be explained by the formation of highly reactive intermediates (**Figure 1**a). In situ-formed intermediates are more reactive than starting monomers and chlorinated solvents, hence self-polymerize to give high-molecular-weight polymers rather than multisubstituted aromatics (Figure S1, Supporting Information). This finding is contrary to some of the reports in the literature, particularly those that claim Scholl's reaction (aromatic–aromatic self-coupling) in chlorinated solvents in the presence of AlCl₃ (Figure S2, Supporting Information).[17a,c–e,g]
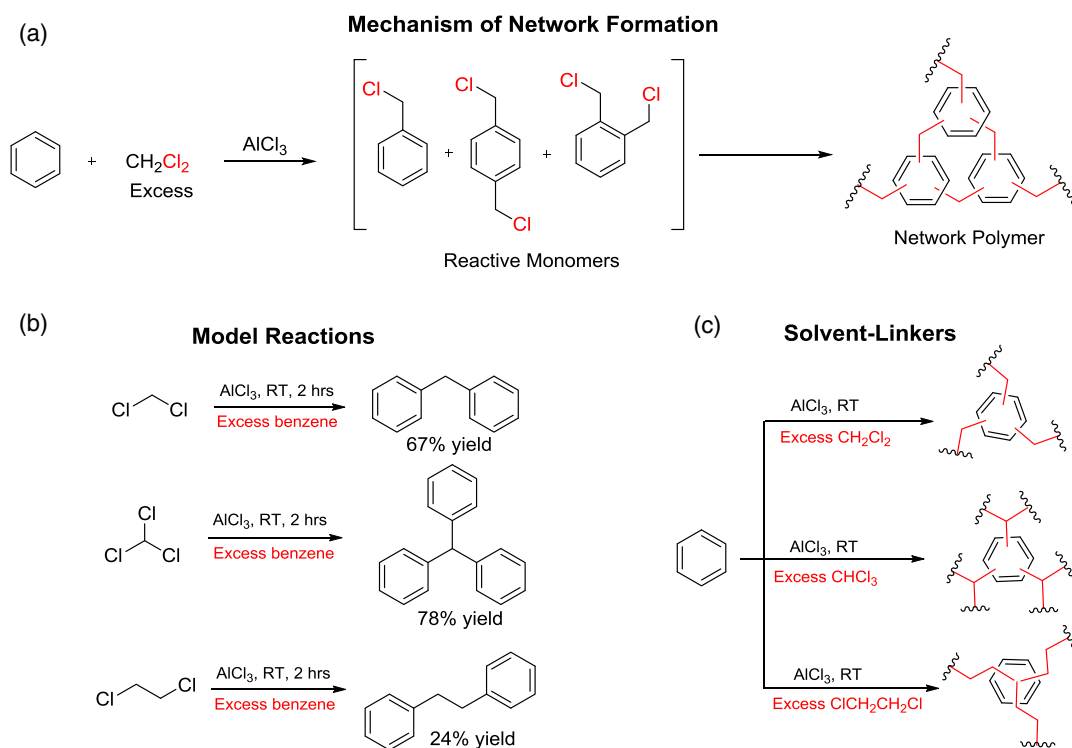

Figure 1. a) Mechanism of network formation. b) Model reaction for the proof of solvent reactivity. c) Formation of three different linkers using DCM, CHCl₃, and DCE.

**ADVANCED
SCIENCE NEWS**

www.advancedsciencenews.com

**ADVANCED
ENERGY & SUSTAINABILITY
RESEARCH**
Open Access

www.advenergysustres.com

To further confirm the reactivity of solvents or aromatic coupling, we conducted model reactions of DCM, CHCl$_3$, and DCE in excess benzene (solvent) and in the presence of anhydrous AlCl$_3$ (Figure 1b). Despite using excess aromatic benzene, no aromatic coupling (e.g., biphenyl, terphenyl) was observed, but FC products, diphenyl methane, triphenyl methane, and 1,2-diphenylethane, were formed (see Figure S5–S10, Supporting Information, for detailed information). In principle, here, alkyl-chlorinated solvents serve as both linkers and solvent. DCM and DCE act as bidentate linkers to give diphenylmethane- and 1,2-diphenylethane-based polymers, whereas chloroform acts as tridentate linker to give triphenylmethane-based polymer (Figure 1c).

Although FC reactions are established to run over [carbocation]$^+$[MetalCl$_x$]$^-$ as active species, Lewis acids such as FeCl$_3$ were recently reported to produce FeCl$_2^+$ in a disproportionation mechanism.[19] When studying this possibility, our trials with FeCl$_3$ in chlorinated solvents failed to produce any insoluble network polymers. At the same time, AlCl$_3$ with stoichiometric chlorinated reagents in nonchlorinated solvents like DMF also did not yield any network polymers, showing that disproportionation paths do not affect the outcome of the network formations in this work.

2.2. Reactivity of Aromatic Monomers and Solvents

We, then, extended this discovery into a range of total 18 different aromatic hydrocarbons in DCM, CHCl$_3$, and DCE solvents, proving that a wide substrate scope is indeed possible (**Table 1**). Among three solvents, CHCl$_3$ formed insoluble polymers with 13 monomers, whereas DCE and DCM formed 9 and 7 polymers, respectively. This can be explained by, due to the electron-withdrawing chlorines, the higher reactivity of CHCl$_3$ and its benzal chloride (benzyl dichloride)-based intermediates. While DCM and benzyl chloride intermediates are more reactive than DCE and (2-chloroethyl)benzene, the longer and flexible DCE can avoid steric hindrance and react with more monomers than DCM.

Among 18 different monomers, three classes of aromatic hydrocarbons, 1) benzene and its methyl-substituted derivatives, 2) heteroatom-containing aromatics, and 3) polycyclic aromatics, were tested (Table 1).

Benzene formed network structures with all three solvents. We believe that inefficient packing and six possible extension positions contribute to this variation. In contrast, methyl-substituted benzenes were not as successful. The mesitylene (1,3,5-trimethyl-benzene), for example, did not give polymer with any of the solvents, and xylene (mixture of isomers) formed a network only with CHCl$_3$. Steric hindrance by methyl groups proves to be a detrimental factor in the formation of a crosslinked structure. For instance, toluene did not yield a polymer in DCM, but longer DCE, where steric hindrance could be avoided, produced an insoluble polymer.

Most heteroatom-containing aromatics are known to be less likely to favor an FC reaction over the aromatic ring.[20] The heteroatom usually chelates with the Lewis acid and the electron-poor adduct deactivates the aromatic rings (Figure S3, Supporting Information). Therefore, pyridine, phenol, aniline, and triphenylphosphine did not give polymer with any of the

Table 1. Reactivity of aromatic monomers with dichloromethane (DCM), chloroform (CHCl$_3$), and 1,2-dichloroethane (DCE). Formed precipitates were isolated and assigned a code name.

Core/linker	CH$_2$Cl$_2$ [yield][a]	CHCl$_3$ [yield][a]	DCE [yield][a]
Benzene	COP-124 (113%)	COP-131 (95%)	COP-150 (137%)
Toluene	No precipitate	COP-132 (23%)	COP-144 (37%)
Xylene (mixture)	No precipitate	COP-133 (18%)	No precipitate
Mesitylene	No precipitate	No precipitate	No precipitate
Phenol	No precipitate	No precipitate	No precipitate
Aniline	No precipitate	No precipitate	No Precipitate
Pyridine	No precipitate	No precipitate	No Precipitate
1,2-dichlorobenzene	No precipitate	COP-143 (57%)	No precipitate
Diphenyl ether	No precipitate	COP-139 (31%)	No precipitate
Diphenyl amine	No precipitate	COP-141 (23%)	COP-151 (63%)
Triphenylamine	No precipitate	COP-142 (58%)	No precipitate
Triphenylphosphine	No precipitate	No precipitate	No precipitate
Triphenylmethane	COP-125 (87%)	COP-136 (84%)	COP-147 (73%)
Tetraphenylmethane	COP-126 (83%)	COP-137 (81%)	COP-148 (67%)
Naphthalene	COP-127 (89%)	COP-134 (73%)	COP-145 (81%)
Biphenyl	COP-128 (93%)	COP-135 (71%)	COP-146 (88%)
Tetraphenyladamantane	COP-129 (71%)	COP-138 (63%)	COP-152 (55%)
1,3,5-Triphenylbenzene	COP-130 (92%)	COP-140 (87%)	COP-149 (103%)

[a]The yields of the polymers were calculated based on the starting aromatic monomers only, crosslinkers were not included.

solvents. Diphenyl ether, diphenyl amine, and triphenylamine formed polymers with highly reactive CHCl$_3$. It is interesting to note that triphenyl amine formed polymer, whereas triphenyl-phosphine did not. We think that is because of the planar (119.6°) geometry of triphenylamine, leading to a weaker interaction between nitrogen and AlCl$_3$, and the higher reactivity of CHCl$_3$ compared with other solvents. On the contrary, this is not true for the triphenylphosphine (TPP) because of its trigonal pyramidal (102.8°) layout, which causes unhindered, strong interaction with Lewis acids (Figure S3, Supporting Information). Hence, no network forms from TPP and halo-organics.

Polycyclic aromatics yielded network structures with all tested solvents. This is in accordance with most of the reported literature; whether it is crystalline MOFs and COFs, or amorphous porous polymers, polycyclic aromatics monomers have been widely used in the formation of porous structures.

2.3. Characterization

The COPs were characterized by Fourier-transform infrared spectroscopy (FTIR), nuclear magnetic resonance (NMR) spectroscopy, elemental composition analysis, scanning electron microscope (SEM), and thermogravimetric analysis (TGA). The characteristic FTIR bands of aromatic C−H bending at 600−900 cm^{-1}, aliphatic C−H bending at 1000−1200 cm^{-1}, aromatic C−C stretching at 1400−1600 cm^{-1}, aliphatic C−H stretching below 3000 cm^{-1}, and aromatic C−H stretching above

ADVANCED
SCIENCE NEWS

www.advancedsciencenews.com

ADVANCED
ENERGY & SUSTAINABILITY
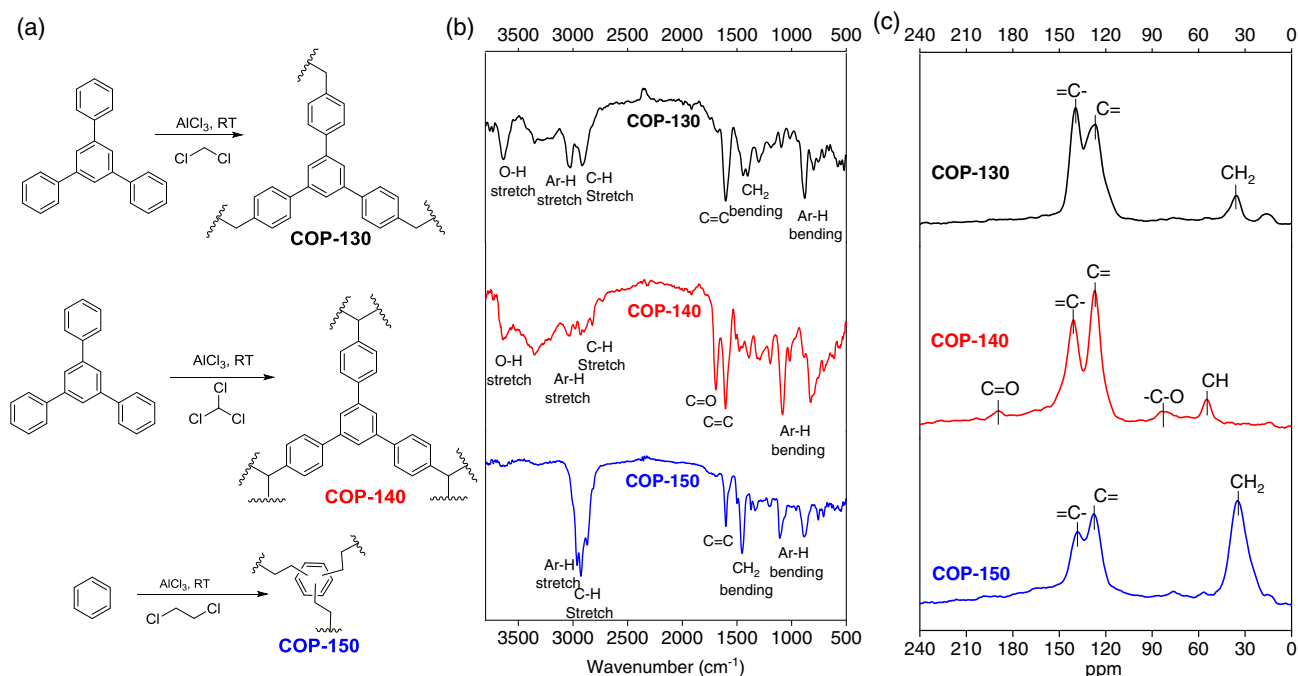RESEARCH
Open Access

www.advenergysustres.com

Figure 2. Characterization of representative COPs from each solvent. a) Reaction schemes for the formation of DCM-linked COP-130, CHCl₃-linked COP-140, and DCE-linked COP-150. b) FTIR spectra of COP-130, COP-140, and COP-150. c) Solid-state ^{13}C NMR spectra of COP-130, COP-140, and COP-150. For the full list of spectra, see Supporting Information.

$3000 \, \text{cm}^{-1}$ support the proposed structures (**Figure 2**). When the spectra of three different solvents were compared, DCE-linked polymers exhibited the strongest aliphatic C−H stretching vibrations, and DCM-linked polymers possess stronger aliphatic C−H stretching vibrations than CHCl₃-linked polymers, showing the characteristics of each linker. The elemental analysis (EA) of COPs was measured after repetitive Soxhlet washings and drying at 120 °C. Apart from high content of carbon and hydrogen, EA also revealed oxygen (**Table 2**). The oxygen was likely introduced through hydrolysis and oxidation of surface-tethered alkyl chlorides during postsynthetic steps (Figure S4, Supporting Information). The CHCl₃-linked COPs contain higher oxygen content (7−10 wt%) than DCM-linked COPs (2−3 wt%) and DCE-linked COPs (1−2 wt%), correlating with the reactivity

of surface chlorides (benzal chloride, benzyl chloride, and (2-chloroethyl)benzene). Hydrolysis and oxidation products were also confirmed by characteristic broad O−H stretching bands at $3300-3500 \, \text{cm}^{-1}$ and carbonyl C=O stretching at $1690 \, \text{cm}^{-1}$ in CHCl₃-linked COPs. There is also a residual aluminum from the catalyst, which is found to be very low (confirmed by Inductively coupled plasma mass spectrometry (ICP-MS)). Solid-state ^{13}C (CP/MAS) NMR spectra of three COPs (one representative from each solvent) are shown in Figure 2c. The spectrum shows mainly two types of carbons, aromatic and aliphatic carbons. The peak at around 140 ppm belongs to substituted aromatic carbons and the one at 127 ppm can be assigned to unsubstituted aromatic carbons. Peaks at 34, 36, and 55 ppm can be attributed to aliphatic carbons

Table 2. EA and BET surface areas of selected ten highly porous COPs.

COPs	Aromatic monomer	Solvent	SA$_{BET}$ [m² g⁻¹]	C [wt%]	H [wt%]	N [wt%]	O [wt%]	Al [wt%]
COP-128	Biphenyl	DCM	616	89.90	5.06	0	2.90	0.74
COP-129	Tetraphenyladamantane	DCM	533	86.19	6.41	0	2.12	0.74
COP-130	1,3,5-Triphenylbenzene	DCM	1685	85.09	4.61	0	3.02	0.72
COP-134	Naphthalene	CHCl₃	719	73.78	3.52	0	9.86	0.77
COP-135	Biphenyl	CHCl₃	711	76.90	4.12	0	7.46	0.83
COP-138	Tetraphenyladamantane	CHCl₃	409	82.51	6.54	0	3.22	0.77
COP-140	1,3,5-Triphenylbenzene	CHCl₃	1219	74.80	4.16	0	7.92	0.81
COP-142	Triphenylamine	CHCl₃	634	68.77	4.04	3.79	8.15	0.76
COP-150	Benzene	DCE	120	83.83	7.46	0	0.79	0.71
COP-152	Tetraphenyladamantane	DCE	524	84.86	6.84	0	1.81	0.72

**ADVANCED
SCIENCE NEWS**
www.advancedsciencenews.com

**ADVANCED
ENERGY & SUSTAINABILITY
RESEARCH**
Open Access
www.advenergysustres.com

of solvent linkers. Aliphatic carbon peaks are in close agreement with model compounds (diphenylmethane, triphenylmethane, 1,2-diphenylethane, see Figure S5–S10, Supporting Information, for NMR spectra). In CHCl$_3$-linked COPs, there are oxidized carbon peaks at 82 ppm (C—O) and 190 ppm (C=O), further supporting the hydrolyzed and oxidized surface species. The TGA of the solvent-linked COPs shows thermal stabilities up to the 400 °C, thanks to their stable C—C-bonded framework (Figure S16–S20, Supporting Information). In CHCl$_3$-linked COPs, due to their hydrophilic surface, there is a 4−10 wt% mass loss up to 120 °C, coming from the desorption of adsorbed water. SEM surface images reveal that COP grains vary from the spherical to flat structure, and the size of spheres varies among COPs (Figure S21–S27, Supporting Information).

2.4. Porosity Analysis

Porosity of COPs was analyzed from Ar adsorption and desorption isotherms at 87 K. The BET surface areas of these materials ranged from nonporous to as high as 1685 m^2 g^{-1} (Table 2). Among 29 COPs, ten of them, mostly from polycyclic aromatic-based structures, exhibited highly porous (>100 m^2 g^{-1}) morphology and those isotherms are shown in **Figure 3**. Tetraphenyladamantane (TPA) consistently gave high porosities with all three solvents. We articulate on the fact that TPA has larger spacing between the phenyl legs of the tetrahedral monomer with rigid, locked, and a saturated hydrocarbon core. This observation is in line with our previous work on Tröger's base networks, where the specific geometry of TPA dictates a highly porous network.[21]

Naphthalene and biphenyl also followed suit, producing networks with DCM and CHCl$_3$. The main exception was at tetraphenylmethane and triphenylmethane mainly due to the intramolecular crosslinking possibilities between freely rotating benzene rings. Surprisingly, 1,3,5-triphenylbenzene led to two of the largest BET surface areas with DCM (COP-130, 1685 m^2 g^{-1}) and with CHCl$_3$ (COP-140, 1219 m^2 g^{-1}). In general, flat aromatic monomers tend to pack π−π stacking, a common mechanism in the formation of ordered COFs.[22] In FC conditions, one would expect this mechanism leading to lower porosity. Most of the DCE-linked COPs showed nonporous structures because of the freely rotating aliphatic dimethylene linkers.

In the isotherms of porous COPs, there is a rapid increase in the low-pressure range (P P_o^{-1} < 0.01) and small hysteresis between adsorption and desorption, indicating both microporous and mesoporous morphology.[23] In particular, the DCM-linked COP-128 and COP-130 showed strong hysteresis. The hysteresis in adsorption and desorption isotherms is widely observed in porous organic polymers such as polymers of intrinsic microporosity (PIMs)[24] and polyimide porous polymers.[25] The origin of hysteresis is associated with swelling of materials,[25a,26] the restricted access to pores,[27] and mesoporous morphology.[28] The differential and cumulative pore size distributions (PSDs) were obtained using nonlocal density functional theory (NLDFT) model (Figure 3). The PSD profile shows that COP-128 and COP-130 possess the highest mesoporous volumes of 51% and 52%, respectively. The CHCl$_3$-linked COPs showed higher microporosity (up to 83%) compared with DCM and DCE (≈50%). We believe that microporosity was formed as a result of higher crosslinking of three dentate CHCl$_3$ compared
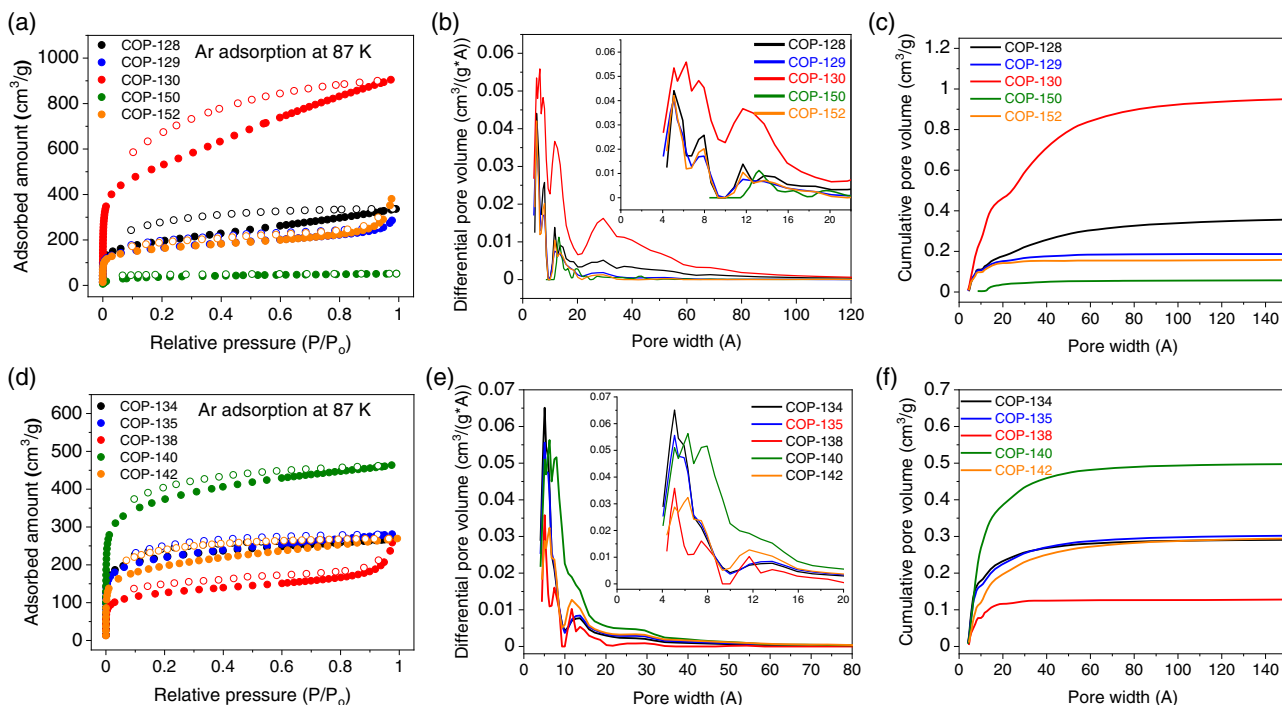

Figure 3. a) Ar adsorption and desorption isotherms at 87 K, b) differential PSDs, and c) cumulative pores volumes of selected five highly porous DCM- and DCE-linked COPs. d) Ar adsorption and desorption isotherms at 87 K, e) differential PSDs, and f) cumulative pore volumes of selected five highly porous CHCl$_3$-linked COPs. For the isotherms of less porous (<100 m^2 g^{-1}) COPs, refer to the Supporting Information.

with two dentate linkers (DCM and DCE). In addition, tetraphenyladamantane-based COPs show rapid increase near saturation pressures because of their macroporosity (Figure 3 and Figure S29f, Supporting Information). We believe that macroporosity comes from the interparticle voids of small particles.[29] As tetraphenyladamantane has low solubility in chlorinated solvents, it led to smaller grains. This is also evident from SEM images (Figure S21 and S27, Supporting Information).

2.5. The CO_2 Adsorption

Due to their high surface areas and low energy regeneration, solid porous adsorbents are being extensively investigated as potential CO_2 sorbents. Herein, we studied CO_2 adsorption properties of COPs at 273 and 298 K up to 1.1 bar and isotherms for porous COPs ($>100\ m^2\ g^{-1}$) are shown in **Figure 4**a–d. As expected, CO_2 adsorption and desorption isotherms showed no hysteresis indicating physisorptive CO_2 binding. At 1.1 bar and 273 K, 1,3,5-triphenylbenzene-based COP-130 (DCM) and COP-140 ($CHCl_3$) exhibited the highest CO_2 uptake performances, with capacities of 4.71 and 4.35 mmol g^{-1}, respectively (**Table 3**). These COPs outperform other FC-based and hydrocarbon-based polymers (Table S2, Supporting Information) such as HCP-1 (2.16 mmol g^{-1}, 1970 $m^2\ g^{-1}$)[12d] and PAF-1 (2.05 mmol g^{-1}, 5600 $m^2\ g^{-1}$).[30] These values are even competing with some oxygen-/nitrogen-rich structures such as BILP-6[11a] (4.79 mmol g^{-1}, 1261 $m^2\ g^{-1}$). Here, unlike other polymerization methods, the reaction of excess solvent linkers leads to richer surface chemistry with dangling species. Unreacted halogens may contribute to CO_2 uptake,[31] although lesser than the remnant oxygens that are introduced by their hydrolysis. We believe that the oxygenated surfaces of COPs produced here are responsible for their superior CO_2
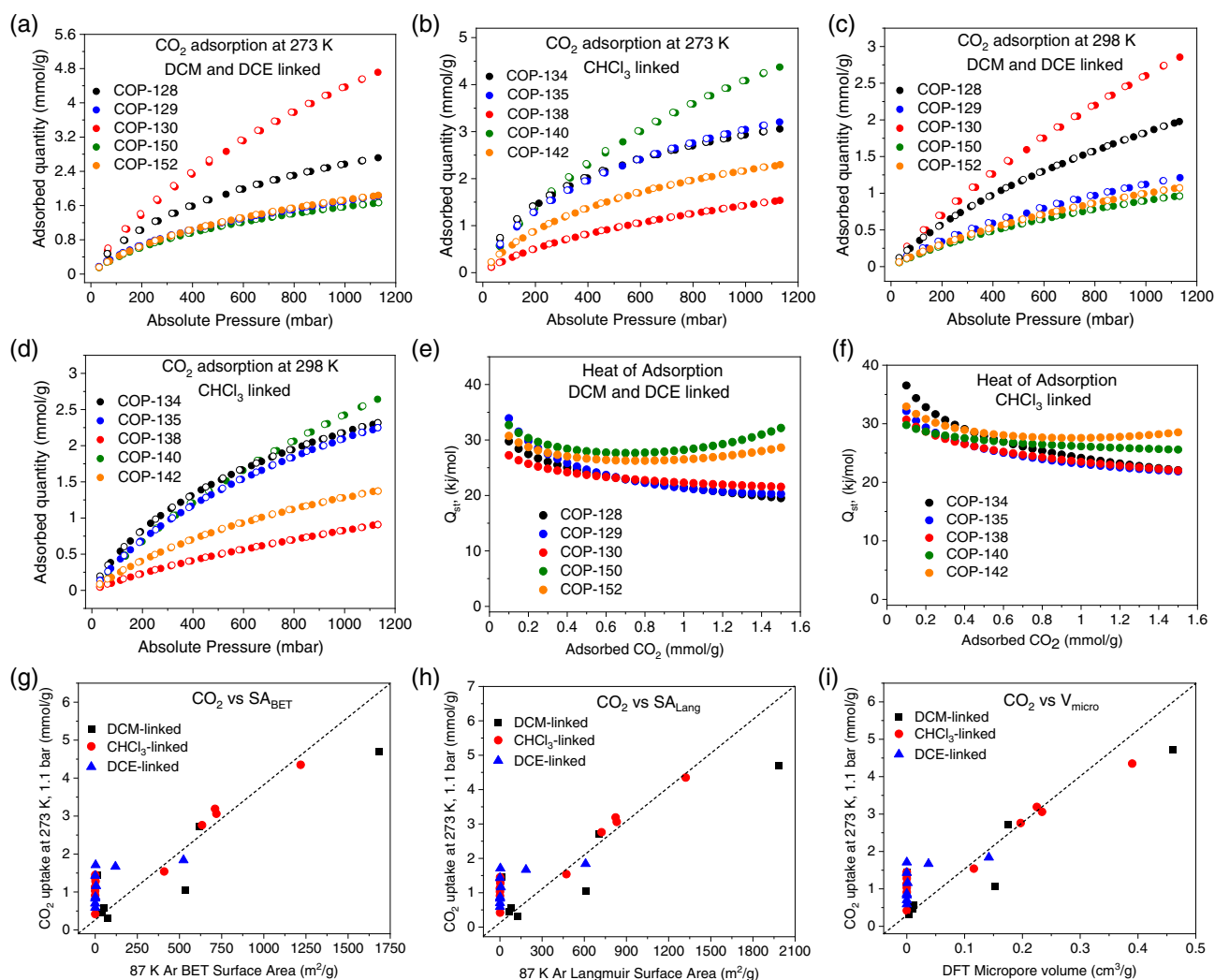

Figure 4. CO_2 adsorption and desorption isotherms of selected five highly porous a) DCM- and DCE-linked COPs at 273 K, b) $CHCl_3$-linked COPs at 273 K, c) DCM- and DCE-linked COPs at 298 K, and d) $CHCl_3$-linked COPs at 298 K. For the isotherms of less-porous ($<100\ m^2\ g^{-1}$) COPs, refer to the Supporting Information. The isosteric heat of adsorption data of five selected highly porous e) DCM- and DCE-linked COPs and f) $CHCl_3$-linked COPs. The correlation of CO_2 uptake capacities (273 K, 1.1 bar) with g) BET surface areas, h) Langmuir surface areas, and i) micropore (<2 nm) volumes, obtained from Ar adsorption isotherms.

**ADVANCED
SCIENCE NEWS**

www.advancedsciencenews.com

**ADVANCED
ENERGY & SUSTAINABILITY
RESEARCH**
Open Access

www.advenergysustres.com

Table 3. Detailed porosity and gas adsorption analysis of all the COPs studied.

COPs	Solvent	Monomer	SA(BET) 87 K Ar [$m^2 g^{-1}$]	SA(Lang) 87 K Ar [$m^2 g^{-1}$]	V_{micro} (<2 nm) [$cm^3 g^{-1}$]	SA(BET) 273 K CO_2 [$m^2 g^{-1}$]	CO_2 uptake 273 K, 1.1 bar [$mmol g^{-1}$]	CH_4 uptake 273 K, 1.1 bar [$mmol g^{-1}$]	H_2 uptake 77 K, 1.1 bar [$mmol g^{-1}$]
COP-124	DCM	Benzene	42	68	0.0092	80	0.464	0.052	0.19
COP-125	DCM	Triphenylmethane	75	124	0.003	56	0.314	0.05	0.413
COP-126	DCM	Tetraphenylmethane	50	78	0.012	73	0.57	0.163	1.49
COP-127	DCM	Naphthalene	12	13	0	182	1.45	0.587	3.28
COP-128	DCM	Biphenyl	616	707	0.175	370	2.72	0.935	5.78
COP-129	DCM	Tetraphenyladamantane	533	614	0.152	147	1.06	0.408	4.2
COP-130	DCM	1,3,5-Triphenylbenzene	1685	1982	0.46	878	4.71	1.28	10
COP-131	CHCl₃	Benzene	2.1	3	0	173	1.28	0.398	1.75
COP-132	CHCl₃	Toluene	0.5	0.7	0	182	1.13	0.347	0.315
COP-133	CHCl₃	Xylene	0.03	0.03	0	132	0.909	0.152	0.003
COP-134	CHCl₃	Naphthalene	719	831	0.234	354	3.06	0.918	5.4
COP-135	CHCl₃	Biphenyl	711	823	0.225	409	3.19	1.11	6.1
COP-136	CHCl₃	Triphenylmethane	0.02	0.04	0	175	1.37	0.426	0.99
COP-137	CHCl₃	Tetraphenylmethane	0.5	0.7	0	4	0.42	0.084	0.08
COP-138	CHCl₃	Tetraphenyladamantane	409	473	0.116	269	1.54	0.524	3.12
COP-139	CHCl₃	Diphenylether	0.94	1.3	0	177	1.45	0.471	3.15
COP-140	CHCl₃	1,3,5-Triphenylbenzene	1219	1322	0.39	707	4.35	1.31	8.42
COP-141	CHCl₃	Diphenylamine	0.05	0.05	0	146	1.03	0.123	0.04
COP-142	CHCl₃	Triphenylamine	634	723	0.197	425	2.76	0.837	4.36
COP-143	CHCl₃	1,2-Dichlorobenzene	0.5	0.6	0	177	1.13	0.337	0.95
COP-144	DCE	Toluene	0.03	0.3	0	115	0.7	0.165	0.03
COP-145	DCE	Naphthalene	0.4	0.7	0	120	0.83	0.191	0.223
COP-146	DCE	Biphenyl	0.3	0.3	0	100	0.59	0.126	0.008
COP-147	DCE	Triphenylmethane	0.12	0.13	0	198	1.43	0.555	3.1
COP-148	DCE	Tetraphenylmethane	2.5	2.7	0	300	1.71	0.45	2.93
COP-149	DCE	1,3,5-Triphenylbenzene	5	6.5	0.0013	178	1.16	0.685	3.6
COP-150	DCE	Benzene	120	185	0.0375	230	1.67	0.561	3.72
COP-151	DCE	Diphenylamine	1.1	1.2	0	128	0.87	0.135	0.006
COP-152	DCE	Tetraphenyladamantane	524	609	0.142	268	1.84	0.722	4.44

performance. The effect of surface chemistry can be estimated from the heat of adsorption (Q_{st}) for CO_2 binding. Q_{st} was calculated from adsorption data at 273 and 298 K using Clausius–Clapeyron's equation. At zero coverage, the Q_{st} values for porous COPs ranged from 27 to 37 kj mol^{-1} (Figure 4e,f). Indeed, as expected these numbers are higher than FC-based HCPs[12d] (20−24 kj mol^{-1}) and aromatic PAFs[30] (15−20 kj mol^{-1}), explaining the better CO_2 uptake performance of these COPs. When different solvent linkers were compared, CHCl₃-linked COPs (30−37 kj mol^{-1}) showed higher Q_{st} values than DCM and DCE (27−34 kj mol^{-1}). This is due to the higher oxygen content of CHCl₃-linked COPs, which result in stronger CO_2 binding.

Apart from surface chemistry, porosity of sorbents also plays an important role in dictating gas adsorption properties. Here, whether they are porous or nonporous, CO_2 adsorption performances of all 29 COPs were measured up to 1.1 bar at 273 K and the data are shown in Table 3. To understand the relation between adsorption capacities and porosity parameters, we plotted CO_2 uptake capacities at 1.1 bar and 273 K against BET surface areas (Figure 4g), Langmuir surface areas (Figure 4h), and micropore volumes (Figure 4i), and they revealed three important findings. First, all plots showed similar trends; no difference was observed among BET surface area, Langmuir surface area, and micropore volume plots. Second, highly porous COP-130 and COP-140, although having best uptake capacities, underperformed with respect to their porosities. This can be explained by their lower number (per surface area) and uneven distribution of surface functional groups on pore surfaces. This is because the higher surface area will result in lower number of oxygenated species per surface area. Third, although porous COPs exhibited relatively a linear trend with porosity parameters, surprisingly, some nonporous polymers showed higher CO_2 adsorption capacities, even competing with higher surface area structures. For instance, nonporous COP-148 (2.5 m^2 g^{-1}) exhibited 1.71 mmol g^{-1} CO_2 uptake at 1.1 bar and 273 K, surpassing porous COP-129 (1.06 mmol g^{-1}, 533 m^2 g^{-1}), COP-138

**ADVANCED
SCIENCE NEWS**

www.advancedsciencenews.com

**ADVANCED
ENERGY & SUSTAINABILITY
RESEARCH**
Open Access

www.advenergysustres.com

(1.54 mmol g^{-1}, 409 m^2 g^{-1}), and COP-150 (1.67 mmol g^{-1}, 120 m^2 g^{-1}). We believe that these COPs possess ultra-microporous cavities inaccessible to larger Ar, but accessible to smaller CO_2 through a quadrupole interaction with surface.[32] To better evaluate the porosities of COPs, BET surface areas were also calculated from CO_2 adsorption isotherms at 273 K and the results are shown in Table 3. While nonporous COPs exhibited higher BET surface areas from CO_2 adsorption than Ar, highly porous COPs showed lower BET surface areas. For instance, less-porous COP-148 (2.5 m^2 g^{-1}) exhibited 300 m^2 g^{-1} using CO_2, but COP-130 (1685 m^2 g^{-1}) showed 878 m^2 g^{-1} (using CO_2), almost half of its surface area when Ar was used.

2.6. The CH$_4$ and H$_2$ Adsorption

Solid porous adsorbents are viable candidates for safely storing and transporting hydrogen (H_2) and methane (CH_4) gases. Therefore, to test our materials, we then switched the gas probe to H_2 and CH_4. The H_2 adsorption and desorption isotherms were measured at 77 K (**Figure 5**). The COPs exhibited high uptake capacities toward H_2 adsorption (Table 3). As in CO_2 adsorption at 1.1 bar, COP-130 and COP-140 showed highest capacities with values 2.02 and 1.70 wt%, respectively. These numbers are among the leading materials in H_2 adsorption (Table S3, Supporting Information). For example, COP-130

stores more H_2 than higher surface area materials such as COF-102 (3530 m^2 g^{-1}, 1.20 wt%)[1b] and PAF-1 (5600 m^2 g^{-1}, 1.50 wt%).[30] To investigate the relation of H_2 uptake and porosity, we plotted the H_2 adsorption capacities of COPs (at 1.1 bar) against their BET surface areas from Ar and CO_2 gases (Figure 5c,d). The plot against Ar surface areas showed similar trend as in Figure 4g (CO_2 plots), with nonporous COPs having higher H_2 uptake capacities than expected. In contrast, most of the H_2 uptake capacities showed fairly linear trend when plotted against CO_2 surface areas. Similar to CO_2, smaller H_2 can access ultra-microporous pores where Ar cannot adsorb. Therefore, it is not surprising to observe a linear trend between CO_2 and H_2 adsorption properties.

The CH_4 isotherms were measured at 273 K, up to 1.1 bar (**Figure 6**). Similarly, COPs exhibited good performance toward CH_4 adsorption, with uptake capacities as high as 1.31 mmol g^{-1} (COP-140) at 273 K, 1.1 bar (Table 3). These values are comparable with important porous materials such as PAF-1 (5600 m^2 g^{-1}, 0.80 mmol g^{-1})[30] and BILP-6 (1261 m^2 g^{-1}, 1.68 mmol g^{-1}) (see Table S4, Supporting Information, for the comparison table). As we did in H_2 adsorption, CH_4 adsorption capacities at 1.1 bar were correlated with BET surface areas from Ar and CO_2 (Figure 6). The CH_4 uptake exhibited similar behavior as in H_2; nonporous COPs showed higher CH_4 capacities when plotted against Ar surface areas but exhibited linear trend against CO_2 surface areas. This is surprising, as CH_4 has a larger kinetic diameter (0.38 nm) than Ar (0.34 nm); hence, one should expect
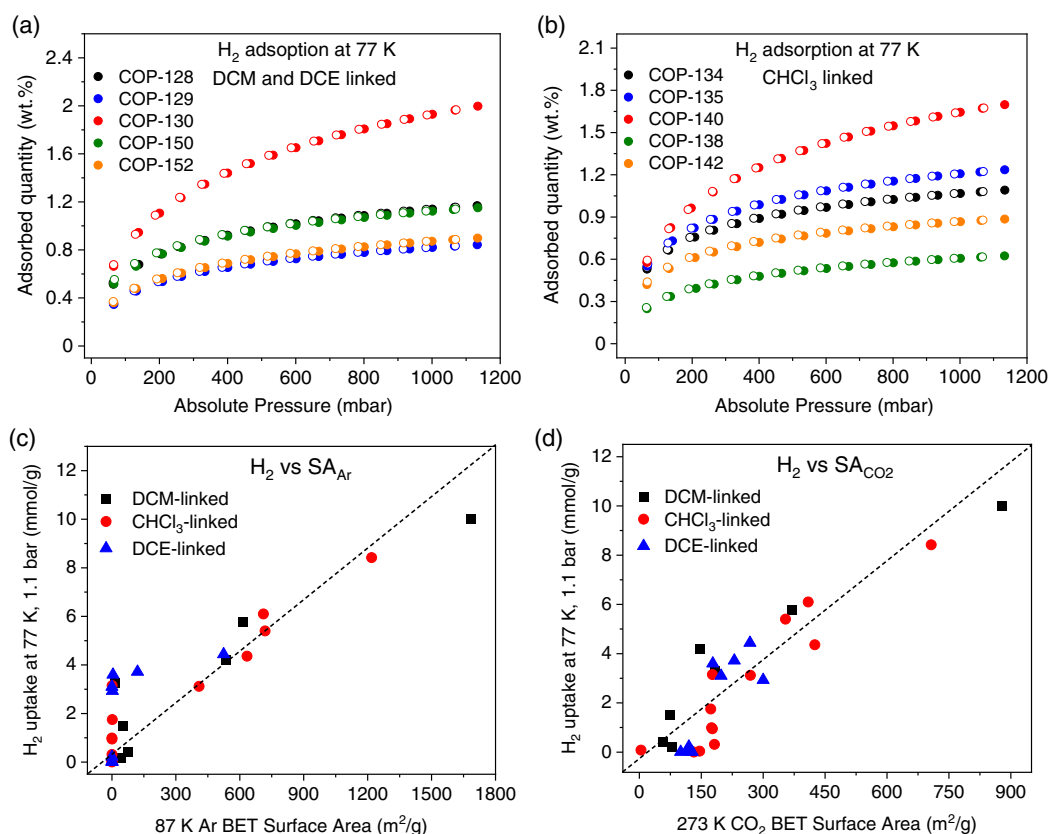

Figure 5. H_2 adsorption and desorption isotherms of selected five highly porous a) DCM- and DCE-linked COPs and b) CHCl$_3$-linked COPs at 77 K up to 1.1 bar. For the isotherms of less-porous (<100 m^2 g^{-1}) COPs, refer to the Supporting Information. The correlation of H_2 uptake capacities (77 K, 1.1 bar) with BET surface areas from c) Ar adsorption and d) CO_2 adsorption isotherms.
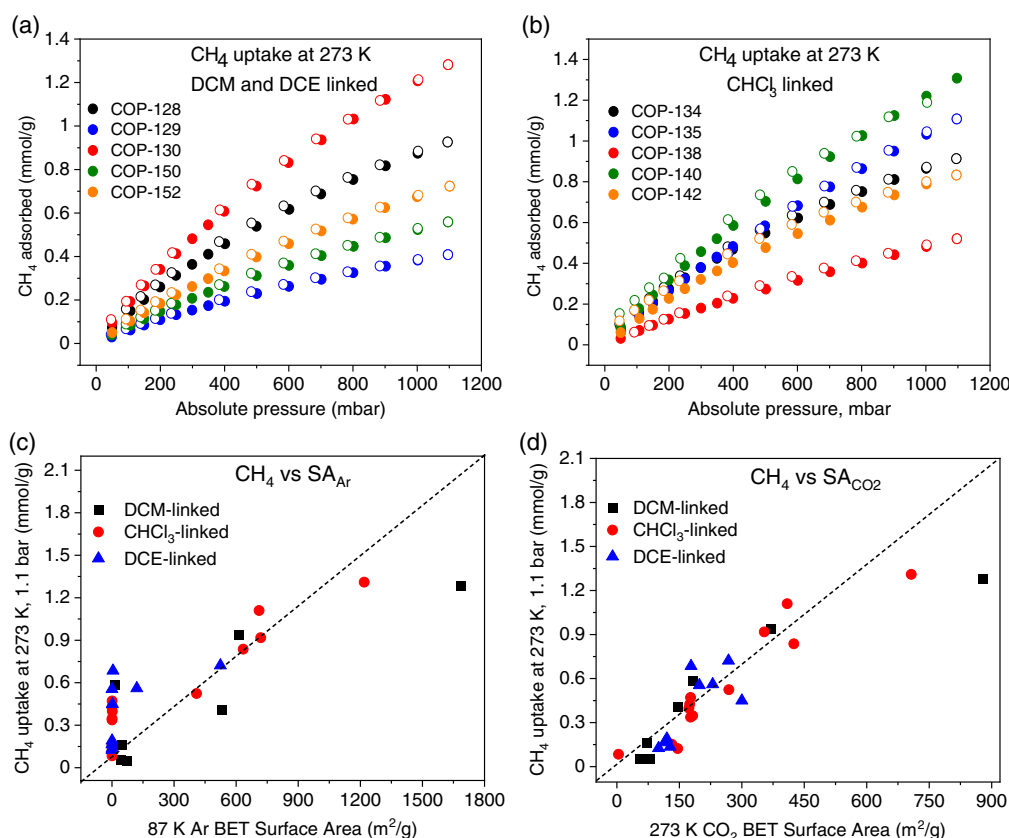
ADVANCED
SCIENCE NEWS
www.advancedsciencenews.com

ADVANCED
ENERGY & SUSTAINABILITY
RESEARCH
Open Access
www.advenergysustres.com

Figure 6. CH_4 adsorption and desorption isotherms of five selected highly porous a) DCM- and DCE-linked COPs and b) $CHCl_3$-linked COPs at 273 K up to 1.1 bar. For the isotherms of less-porous ($100 \, m^2 \, g^{-1}$) COPs, refer to the Supporting Information. The correlation of CH_4 uptake capacities (273 K, 1.1 bar) with BET surface areas from c) Ar adsorption and d) CO_2 adsorption isotherms.

linear correlation between CH_4 capacities and BET surface areas from Ar. However, linear trend with CO_2 surface areas indicates that CH_4 can access ultra-micropores where only H_2 and CO_2 can fit. One possible explanation is that these COPs possess flexible frameworks with affinity toward CH_4 adsorption. Several studies reported CH_4-specific pore expansion of porous materials to allow higher uptake capacity.[18a,33] Previously, we showed that at high pressures, flexible COP-150 and COP-148 can expand and store high amount of CH_4.[18a] These COPs feature methanophilic aromatic and aliphatic hydrocarbon framework with alkyl bridges to allow rotational freedom enabling structural expansion with external stimuli. Although the COPs studied here show exceptional promise toward CH_4 and H_2 uptake, they were only tested up to 1.1 bar. As CH_4 and H_2 are often stored at high pressures (up to 100 bar), high-pressure gas uptake analysis is needed for better assessment of materials performance.

3. Conclusion

In conclusion, we have discovered that chlorinated solvents can be used as linkers in the formation of porous network polymers with aromatic compounds in the presence of $AlCl_3$. Using the new method, a series of 29 different porous polymers were prepared by varying 18 different aromatic monomers in dichloromethane, chloroform, 1,2-dichloroethane. Dichloromethane and

1,2-dichloroethane act as bidentate linkers to produce diphenylmethane and 1,2-diphenylethane-based polymers, respectively, but chloroform acts as tridentate linker to yield triphenylmethane-based polymers. Produced COPs featured from nonporous to highly porous structures. Two of the best performing polymers are 1,3,5-triphenylbenzene-based COP-130 and COP-140 with BET surface areas of 1685 and 1219 $m^2 \, g^{-1}$, respectively. The highly porous COPs showed excellent gas uptake properties toward CO_2 (up to 4.71 $mmol \, g^{-1}$, 273 K, 1.1 bar), CH_4 (up to 1.31 $mmol \, g^{-1}$, 273 K, 1.1 bar), and H_2 (up to 2.02 wt%, 77 K, 1.1 bar). The H_2 and CH_4 adsorption capacities showed linear correlation with BET surface areas using CO_2, rather than Ar gas surface areas. This easy and cheap method makes these polymers potential candidates for gas separation and storage applications in industrial scale. Considering the scalable and inexpensive synthesis, COPs studied here show great promise for CO_2, H_2, and CH_4 uptake.

4. Experimental Methods

Materials: Dichloromethane (DCM, 99.5%), chloroform ($CHCl_3$, 99.5%), 1,2-dichloroethane (DCE, 99.0%), benzene (99.5%), toluene (99.7%), xylene (99.5%), 1,2-dichlorobenzene (99.0%), pyridine (99.0%), phenol (99.0%), aniline (99.0%), naphthalene (99.0%), anhydrous iron (III) chloride (98%), and methanol (99.0%) were purchased from Samchun Pure Chemicals, Korea. Diphenyl ether (99.0%), diphenylamine

ADVANCED
SCIENCE NEWS
www.advancedsciencenews.com

ADVANCED
ENERGY & SUSTAINABILITY
RESEARCH
Open Access
www.advenergysustres.com

(99.0%), triphenylamine (98%), triphenylphosphine (99.0%), and deuterated chloroform (99.96% deuterium and contains tetramethylsilane) were purchased from Sigma Aldrich, USA. Triphenylmethane, tetraphenylmethane (98%), and 1,3,5-triphenylbenzene (99%) were purchased from Alfa Aesar, Korea. Mesitylene (97%) and biphenyl (99%) were purchased from Acros Organics, Korea. 1-Bromoadamantane and 2-bromo-2-methylpropane were purchased from Tokyo Chemical Industry (TCI), Japan. Aluminum chloride (95%) and phosphorus pentoxide (P_2O_5) were purchased from Junsei Chemicals, Korea. Dichloromethane, chloroform, 1,2-dichloroethane, and 1,2-dichlorobenzene were distilled over P_2O_5 under nitrogen atmosphere (where they are referred to as a dry solvent). All the solvents were used without purification when they were used for washing purposes or as Soxhlet extraction solvents. Physical properties and safety information of all the chemicals used in this study are shown in Table S1, Supporting Information.

Characterization: FTIR with attenuated total reflectance (FTIR-ATR) was done using Shimadzu IRTracer, Gladi-ATR 10 model Fourier-transform infrared spectrometer. Solid-state CP/MAS ^{13}C NMR spectra of COPs were measured by Bruker Avance III 400 WB NMR spectrometer. The elemental composition of polymers was measured using a combustion (C/H/N/S and O) analyzer and Al content was obtained from ICP-MS measurements after digesting polymers in solution. Prior to ICP-MS measurements, the polymers were digested in concentrated 60 wt% HNO_3 solution. About 5 mg of polymer sample was added to 1 mL of nitric acid and the mixture was heated to 80 °C and sonicated for 30 min. TGA analyses were conducted on a Shimadzu DTG-60A by heating the samples from 30 °C up to 800 °C at a rate of 10 °C min^{-1} under N_2. Scanning electron microscope (SEM) images were taken by field-emission SEM, Magellan400, FEI Company, USA. Porosity analysis of the solvent-linked COPs was conducted with the Micromeritics ASAP 2020-accelerated surface area and porosimetry analyzer. Samples were degassed at 150 °C for 6 h under vacuum. The Ar adsorption and desorption isotherms at 87 K were obtained to give pore parameters, including BET (at $P\ P_o^{-1} = 0.01-0.25$) surface area and Langmuir (at $P\ P_o^{-1} = 0.01-0.25$) surface area, PSD, and pore volume. The PSDs of solvent-linked COPs were calculated from Ar adsorption isotherms by the NLDFT method using a slit pore model. Total pore volumes of COPs were calculated at $P\ P_o^{-1} = 0.99$. Micropore volumes of COPs were extracted from NLDFT cumulative PSDs under 2 nm. The CO_2 adsorption and desorption isotherms were measured up to 1.1 bar at 273 and 298 K, using a volumetric system (ASAP 2020, Micromeritics Inc., USA). The CH_4 and H_2 adsorption and desorption isotherms were measured up to 1.1 bar at 273 and 77 K, respectively, using a volumetric system (ASAP 2020, Micromeritics Inc., USA). The temperature during adsorption and desorption was kept constant using a circulator. Before the gas adsorption measurements, all samples were properly dried at 120 °C under vacuum for 12 h and degassed under vacuum at 150 °C for 6 h.

Synthesis: Tetraphenyladamantane was prepared by a reported procedure,[34] and all other chemicals were commercially available. Dichloromethane, chloroform, and 1,2-dichloroethane solvents were distilled over P_2O_5 under inert gas when they were referred to as dry. Other chemicals were used without further purification. Solvent-linked COPs were synthesized under inert conditions by mixing ≈1 g (or 1 mL) aromatic monomer with 2–4 molar equivalent (depending on the monomer) of $AlCl_3$ in 20 mL of dry chlorinated solvent in the 30 mL glass vial (Caution: HCl might build up pressure in the vial). The reaction mixture was stirred for 48 h at room temperature under inert conditions. Throughout the synthesis, the color of the solution mixture slowly turned to red and then to black (Caution: $AlCl_3$ and methanol reaction is highly exothermic). The obtained solid was filtered and washed with methanol and chloroform in Soxhlet extractor. The resulting solid was dried under vacuum at 120 °C. For the detailed procedures of each COP polymer, refer to the Supplementary Information.

Supporting Information

Supporting Information is available from the Wiley Online Library or from the author.

Conflict of Interest

The authors declare no conflict of interest.

Data Availability Statement

Research data are not shared.

[1] a) S. Ma, H.-C. Zhou, *Chem. Commun.* **2010**, *46*, 44; b) H. Furukawa, O. M. Yaghi, *J. Am. Chem. Soc.* **2009**, *131*, 8875; c) P. M. Budd, K. J. Msayib, C. E. Tattershall, B. S. Ghanem, K. J. Reynolds, N. B. McKeown, D. Fritsch, *J. Memb. Sci.* **2005**, *251*, 263; d) W. Guo, S. M. Mahurin, R. R. Unocic, H. Luo, S. Dai, *Nano Lett.* **2020**, *20*, 7995.

[2] a) E. M. Dias, C. Petit, *J. Mater. Chem. A* **2015**, *3*, 22484; b) H. A. Patel, M. S. Yavuz, C. T. Yavuz, *RSC Adv.* **2014**, *4*, 24320; c) Z. Xu, Q. Zhang, H. H. P. Fang, *Crit. Rev. Environ. Sci. Technol.* **2003**, *33*, 363; d) Z. Dong, C. Zhang, H. Peng, J. Gong, H. Wang, Q. Zhao, J. Yuan, *Mater. Horizons* **2020**, *7*, 2683.

[3] a) I. Pulko, J. Wall, P. Krajnc, N. R. Cameron, *Chem. Eur. J.* **2010**, *16*, 2350; b) Y. Zhang, L. Zhao, P. K. Patra, J. Y. Ying, *Adv. Synth. Catal.* **2008**, *350*, 662; c) C. E. Chan-Thaw, A. Villa, P. Katekomol, D. Su, A. Thomas, L. Prati, *Nano Lett.* **2010**, *10*, 537; d) M. Garai, V. Rozyyev, Z. Ullah, A. Jamal, C. T. Yavuz, *APL Mater.* **2019**, *7*, 111102; e) Z. Zhang, S. Yao, X. Hu, F. Okejiri, K. He, P. Liu, Z. Tian, V. P. Dravid, J. Fu, X. Zhu, S. Dai, *Adv. Sci.* **2021**, *8*, 2001493.

[4] a) O. M. Yaghi, M. O'Keeffe, N. W. Ockwig, H. K. Chae, M. Eddaoudi, J. Kim, *Nature* **2003**, *423*, 705; b) J. L. C. Rowsell, O. M. Yaghi, *Microporous Mesoporous Mater.* **2004**, *73*, 3; c) V. Rozyyev, C. T. Yavuz, *Chem* **2017**, *3*, 719.

[5] a) A. P. Côté, A. I. Benin, N. W. Ockwig, M. O'Keeffe, A. J. Matzger, O. M. Yaghi, *Science* **2005**, *310*, 1166; b) F. J. Uribe-Romo, J. R. Hunt, H. Furukawa, C. Klöck, M. O'Keeffe, O. M. Yaghi, *J. Am. Chem. Soc.* **2009**, *131*, 4570; c) M. Martínez-Abadía, C. T. Stoppiello, K. Strutynski, B. Lerma-Berlanga, C. Martí-Gastaldo, A. Saeki, M. Melle-Franco, A. N. Khlobystov, A. Mateo-Alonso, *J. Am. Chem. Soc.* **2019**, *141*, 14403.

[6] a) D. Thirion, Y. Kwon, V. Rozyyev, J. Byun, C. T. Yavuz, *Chem. Mater.* **2016**, *28*, 5592; b) D. Thirion, V. Rozyyev, J. Park, J. Byun, Y. Jung, M. Atilhan, C. T. Yavuz, *Phys. Chem. Chem. Phys.* **2016**, *18*, 14177.

[7] a) M. P. Tsyurupa, V. A. Davankov, *React. Funct. Polym.* **2002**, *53*, 193; b) M. Negre, M. Bartholin, A. Guyot, *Angew. Makromol. Chem.* **1979**, *80*, 19.

[8] a) J.-X. Jiang, A. I. Cooper, in *Functional Metal-Organic Frameworks: Gas Storage, Separation and Catalysis* (Ed: M. Schröder), Springer Berlin Heidelberg, Berlin, Heidelberg **2010**, pp. 1–33; b) J. He, Y. Wang, J. Yuan, C. Liu, C. Pan, Z. Weng, X. Tang, Y. Liu, G. Yu, *Appl. Mater. Today* **2020**, *18*, 100507.

[9] a) T. Ben, H. Ren, S. Ma, D. Cao, J. Lan, X. Jing, W. Wang, J. Xu, F. Deng, J. M. Simmons, S. Qiu, G. Zhu, *Angew. Chem., Int. Ed.* **2009**, *48*, 9457; b) T. Ben, S. Qiu, *CrystEngComm* **2013**, *15*, 17.

[10] a) W. Lu, Z. Wei, D. Yuan, J. Tian, S. Fordham, H.-C. Zhou, *Chem. Mater.* **2014**, *26*, 4589; b) W. Lu, D. Yuan, D. Zhao, C. I. Schilling, O. Plietzsch, T. Muller, S. Bräse, J. Guenther, J. Blümel, R. Krishna, Z. Li, H.-C. Zhou, *Chem. Mater.* **2010**, *22*, 5964.

[11] a) M. G. Rabbani, H. M. El-Kaderi, *Chem. Mater.* **2012**, *24*, 1511; b) Y. Cui, Y. Zhao, T. Wang, B. Han, *Chin. J. Chem.* **2015**, *33*, 131.

[12] a) F. Bai, B. Huang, X. Yang, W. Huang, *Polymer* **2007**, *48*, 3641; b) A. Deryło-Marczewska, J. Goworek, W. Zgrajka, *Langmuir* **2001**, *17*, 6518; c) B. Li, R. Gong, W. Wang, X. Huang, W. Zhang, H. Li, C. Hu, B. Tan, *Macromolecules* **2011**, *44*, 2410; d) C. F. Martin, E. Stockel, R. Clowes, D. J. Adams, A. I. Cooper, J. J. Pis, F. Rubiera, C. Pevida, *J. Mater. Chem.* **2011**, *21*, 5475; e) J. Goworek, A. Deryło-Marczewska, W. Stefaniak, W. Zgrajka, R. Kusak, *Mater. Chem. Phys.* **2003**, *77*, 276.

[13] C. A. C. Friedel, *Comptes Rendus de l'Aceademie des Sciences*, Vol. *84*, Paris **1877**, pp. 1392–1450.

[14] V. A. Davankov, M. P. Tsyurupa, *React. Polym.* **1990**, *13*, 27.

[15] a) X. Song, W. Zhu, Y. Yan, H. Gao, W. Gao, W. Zhang, M. Jia, *J. Mol. Catal., A: Chem.* **2016**, *413*, 32; b) R. Li, Z. J. Wang, L. Wang, B. C. Ma, S. Ghasimi, H. Lu, K. Landfester, K. A. I. Zhang, *ACS Catal.* **2016**, *6*, 1113.

[16] a) M. A. Beckett, D. S. Brassington, S. J. Coles, M. B. Hursthouse, *Inorg. Chem. Commun.* **2000**, *3*, 530; b) J. M. Hogg, L. C. Brown, K. Matuszek, P. Latos, A. Chrobok, M. Swadźba-Kwaśny, *Dalton Trans.* **2017**, *46*, 11561; c) M. Chen, Y. Luo, G. Li, M. He, J. Xie, H. Li, X. Yuan, *Korean J. Chem. Eng.* **2009**, *26*, 1563.

[17] a) L. Meng, X. Zou, S. Guo, H. Ma, Y. Zhao, G. Zhu, *ACS Appl. Mater. Interfaces* **2015**, *7*, 15561; b) H. Lim, M. C. Cha, J. Y. Chang, *Macromol. Chem. Phys.* **2012**, *213*, 1385; c) Q. Luo, C. Zhao, G. Liu, H. Ren, *Sci. Rep.* **2016**, *6*, 20311; d) S. Wang, L. Tan, C. Zhang, I. Hussain, B. Tan, *J. Mater. Chem. A* **2015**, *3*, 6542; e) B. Li, Z. Guan, X. Yang, W. D. Wang, W. Wang, I. Hussain, K. Song, B. Tan, T. Li, *J. Mater. Chem. A* **2014**, *2*, 11930; f) G. Liu, Y. Wang, C. Shen, Z. Ju, D. Yuan, *J. Mater. Chem. A* **2015**, *3*, 3051; g) L. Li, K. Cai, P. Wang, H. Ren, G. Zhu, *ACS Appl. Mater. Interfaces* **2015**, *7*, 201; h) L. Li, H. Ren, Y. Yuan, G. Yu, G. Zhu, *J. Mater. Chem. A* **2014**, *2*, 11091.

[18] a) V. Rozyyev, D. Thirion, R. Ullah, J. Lee, M. Jung, H. Oh, M. Atilhan, C. T. Yavuz, *Nat. Energy* **2019**, *4*, 604; b) P. Jorayev, I. Tashov, V. Rozyyev, T. S. Nguyen, N. A. Dogan, C. T. Yavuz, *ChemSusChem* **2020**, *13*, 6433.

[19] a) R. Tomifuji, K. Maeda, T. Takahashi, T. Kurahashi, S. Matsubara, *Org. Lett.* **2018**, *20*, 7474; b) T. Saito, Y. Nishimoto, M. Yasuda, A. Baba, *J. Org. Chem.* **2006**, *71*, 8516.

[20] R. Dawson, T. Ratvijitvech, M. Corker, A. Laybourn, Y. Z. Khimyak, A. I. Cooper, D. J. Adams, *Polym. Chem.* **2012**, *3*, 2034.

[21] J. Byun, S.-H. Je, H. A. Patel, A. Coskun, C. T. Yavuz, *J. Mater. Chem. A* **2014**, *2*, 12507.

[22] a) S. Wan, F. Gándara, A. Asano, H. Furukawa, A. Saeki, S. K. Dey, L. Liao, M. W. Ambrogio, Y. Y. Botros, X. Duan, S. Seki, J. F. Stoddart, O. M. Yaghi, *Chem. Mater.* **2011**, *23*, 4094; b) E. L. Spitler, B. T. Koo, J. L. Novotney, J. W. Colson, F. J. Uribe-Romo, G. D. Gutierrez, P. Clancy, W. R. Dichtel, *J. Am. Chem. Soc.* **2011**, *133*, 19416; c) M. Martínez-Abadía, A. Mateo-Alonso, *Adv. Mater.* **2020**, *32*, 2002366.

[23] a) K. S. W. Sing, *Pure Appl. Chem.* **1985**, *57*, 603; b) J. Rouquerol, D. Avnir, C. W. Fairbridge, D. H. Everett, J. M. Haynes, N. Pernicone, J. D. F. Ramsay, K. S. W. Sing, K. K. Unger, *Pure Appl. Chem.* **1994**, *66*, 1739.

[24] M. Heuchel, D. Fritsch, P. M. Budd, N. B. McKeown, D. Hofmann, *J. Memb. Sci.* **2008**, *318*, 84.

[25] a) J. Weber, M. Antonietti, A. Thomas, *Macromolecules* **2008**, *41*, 2880; b) N. Ritter, I. Senkovska, S. Kaskel, J. Weber, *Macromolecules* **2011**, *44*, 2025.

[26] J. Weber, J. Schmidt, A. Thomas, W. Böhlmann, *Langmuir* **2010**, *26*, 15650.

[27] J. Jeromenok, J. Weber, *Langmuir* **2013**, *29*, 12982.

[28] a) M. Thommes, B. Smarsly, M. Groenewolt, P. I. Ravikovitch, A. V. Neimark, *Langmuir* **2006**, *22*, 756; b) K. Morishige, *Adsorption* **2008**, *14*, 157; c) G. A. Tompsett, L. Krogh, D. W. Griffin, W. C. Conner, *Langmuir* **2005**, *21*, 8214.

[29] a) S. Jung, S. Ehlert, M. Pattky, U. Tallarek, *J. Chromatogr. A* **2010**, *1217*, 696; b) H. Guan, G. Guiochon, *J. Chromatogr. A* **1996**, *731*, 27.

[30] T. Ben, C. Pei, D. Zhang, J. Xu, F. Deng, X. Jing, S. Qiu, *Energy Environ. Sci.* **2011**, *4*, 3991.

[31] R. Ullah, M. Atilhan, B. Anaya, S. Al-Muhtaseb, S. Aparicio, D. Thirion, C. T. Yavuz, *RSC Adv.* **2016**, *6*, 66324.

[32] a) K. C. Kim, T.-U. Yoon, Y.-S. Bae, *Microporous Mesoporous Mater.* **2016**, *224*, 294; b) F. Ambroz, T. J. Macdonald, V. Martis, I. P. Parkin, *Small Methods* **2018**, *2*, 1800173.

[33] a) S. Krause, V. Bon, I. Senkovska, U. Stoeck, D. Wallacher, D. M. Többens, S. Zander, R. S. Pillai, G. Maurin, F.-X. Coudert, S. Kaskel, *Nature* **2016**, *532*, 348; b) J. A. Mason, J. Oktawiec, M. K. Taylor, M. R. Hudson, J. Rodriguez, J. E. Bachman, M. I. Gonzalez, A. Cervellino, A. Guagliardi, C. M. Brown, P. L. Llewellyn, N. Masciocchi, J. R. Long, *Nature* **2015**, *527*, 357.

[34] H. Newman, *Synthesis* **1972**, *1972*, 692.